J. Fluid Mech. (2000), *vol.* 408, *pp.* 323–345. Printed in the United Kingdom

The mean velocity profile of turbulent boundary layers with system rotation

By T. B. NICKELS[1] AND P. N. JOUBERT[2]

[1]Department of Engineering, Trumpington Street, Cambridge CB2 1PZ, UK

[2]Department of Mechanical Engineering, University of Melbourne, Parkville 3052, Australia

(Received 10 December 1998 and in revised form 10 December 1999)

This paper examines changes in the mean velocity profiles of turbulent boundary layers subjected to system rotation. Analysis of the data from several studies conducted in the large rotating wind tunnel at the University of Melbourne shows the existence of a universal linear correction to the velocity profile in the logarithmic region. The appropriate parameters relevant to rotation are derived and correlations are found between the parameters. Flows with adverse pressure gradients, zero pressure gradients and secondary flows are examined and all appear to exhibit the universal linear correction, suggesting that it is robust.

1. Introduction

The study of the effects of system rotation on turbulent boundary layers is of considerable practical importance. The performance of fans, pumps and turbines is directly affected by the development of the boundary layers on the moving surfaces. These boundary layers are subjected to Coriolis forces that arise due to the rotating frame of reference in which they develop. In order to predict and improve the performance of such devices it is necessary to understand the effects of Coriolis forces on turbulent boundary layers.

A large rotating wind tunnel situated at the University of Melbourne has been used to study the effect of spanwise rotation on turbulent boundary layers under various conditions and has resulted in a significant database on these effects. It has been observed in these (and other) studies that the mean velocity profiles of the boundary layers are significantly altered by rotation. In this paper the data from the experiments are re-examined in order to determine the nature of the change to the velocity profiles. It will be shown that the modification of the profiles can be explained by the addition of a universal linear correction that applies in the usual logarithmic region.

Bradshaw (1969) suggested a similar correction based on an analogy between both curvature and rotation effects with the effect of buoyancy in turbulent flows. By drawing this analogy he was then able to use empirical formulae from studies of atmospheric flows to predict the effects of curvature and rotation on turbulent boundary layers. He used the Monin–Oboukhov formula which relates the Richardson number to a change in mixing length. This leads to a linear correction to the logarithmic profile. In order to estimate the values of the gradient of the correction for rotating flows he used the data of Halleen & Johnston (1967) which were measured in a rotating duct flow. Unfortunately, there were insufficient data in the appropriate region and Bradshaw (1969) admitted that the values of the constants derived from

these data were not quantitatively useful. Using the analogy and empirical results from atmospheric boundary layers he also suggested that the gradient of the extra linear term would be different for the 'stabilized' and 'destabilized' layers.

Galperin & Mellor (1991) have also analysed boundary layers with streamline curvature and spanwise rotation using a turbulence model with algebraic equations for the Reynolds stresses and differential equations for the turbulence energy and length scale. Using a local equilibrium approximation they showed that the flow depends on a single stability parameter. Applying the analysis to the 'constant flux layer', and assuming that the mixing length in this region is proportional to κy, they then derive an equation for the mean velocity profile. To first order this involves the usual logarithmic law with a linear correction similar to that suggested here.

Litvai & Preszler (1969) suggested a different modification to the mean velocity profiles. Their proposal is that the von Kármán constant, κ, changes with rotation. The analysis to support this suggestion is based on a loose analogy with a spring–mass system that the authors of the present paper do not find very convincing. Nevertheless, Watmuff, Witt & Joubert (1985) showed that with a certain choice of constants the modification appeared to fit their data. A comparison of this modification with the linear correction is given in Appendix A. Galperin & Mellor (1991) are similarly unconvinced by this approach and comment that: "...departures from the conventional law-of-the-wall are themselves not logarithmic and cannot be modelled merely by a change in κ."

The purpose of this paper is to examine the form of the mean velocity profiles in turbulent boundary layers subjected to system rotation using dimensional analysis and then to examine the (quite large amount of) available data in the light of this analysis. The data considered consist of over one hundred mean velocity profiles from three different studies conducted at Melbourne plus a few more, measured specifically for this paper, in a flow with a strong pressure gradient.

2. Apparatus

All of the data examined in this paper were measured in the large rotating wind tunnel at the University of Melbourne. Although the apparatus has been described in detail in several of the publications cited, a brief description follows. Figure 1 shows the configuration. As shown, a two-stage axial flow fan driven by a DC motor blows air through a coupling along the axis of rotation of the test section. This flow is turned (using turning vanes) through three corners, passes through a settling chamber with honeycomb, screens and a contraction and then exits through the working section in a radial direction. The boundary layers on both vertical walls are tripped using 1.2 mm trip wires located approximately 30 mm downstream of the contraction exit. The size of the trip was chosen in accordance with the recommendations of Erm (1988). The boundary layer to be studied develops on one of the vertical walls of the working section (the 'measurement wall') and an automated traverse is mounted on the opposite wall. The traverse can be mounted at various streamwise (x) positions to study the development of the boundary layer and can move the probe normal to the wall (y-direction) and in the spanwise direction (z-direction). The two vertical walls may be adjusted to impose a pressure gradient in the working section. The sense of rotation of the working section can be reversed so as to reverse the direction of the Coriolis force on the measurement wall. This removes the necessity of measuring the boundary layers on both walls. The convention used here for indicating the direction of rotation is to describe the wall on which the pressure is reduced as the suction-side

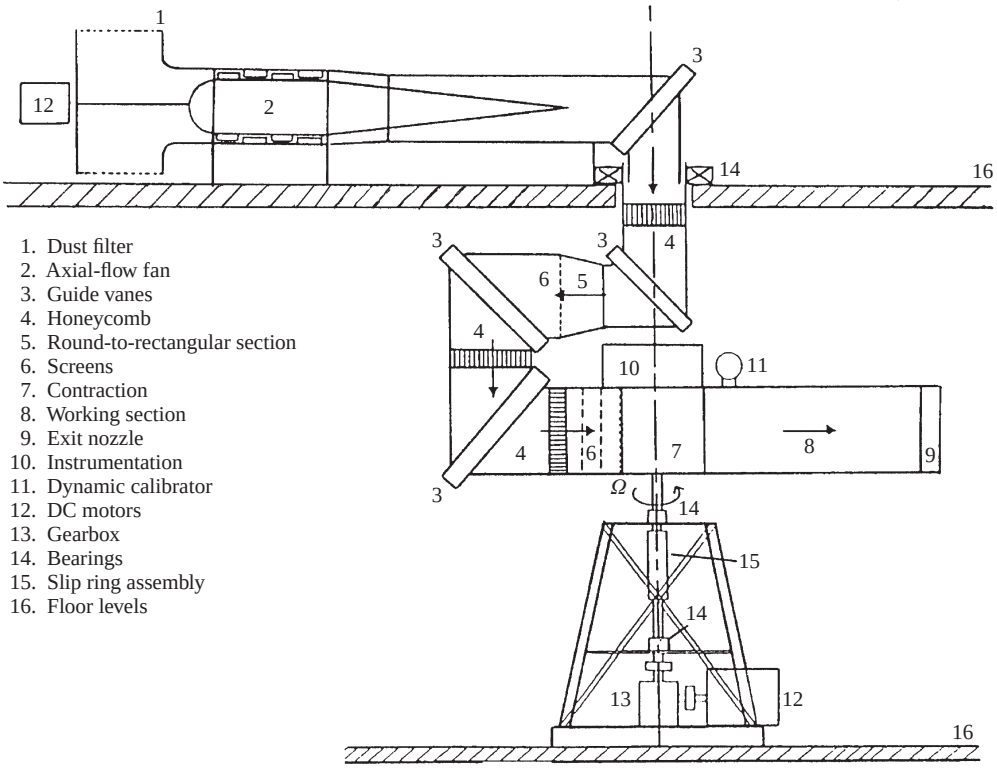

FIGURE 1. Elevation of rotating wind tunnel used for the results presented.

wall, and the wall on which the pressure is increased as the pressure-side wall. The suction-side wall is also referred to as the stabilized side and the pressure-side wall as the destabilized side from the results of stability analysis. The sense of rotation is considered as positive for the suction-side boundary layer.

Static pressure measurements have been made using wall pressure tappings. Velocity measurements were made using a Pitot tube of 1 mm diameter.

The skin friction was measured using a Preston tube of 1 mm diameter. In order to check for errors due to rotation, different diameter Preston tubes were used to measure the skin friction (d =1.0, 1.4 and 1.8 mm). These sizes corresponded to $15 < d^+ < 40$ (where $d^+ = dU_\tau/\nu$) and it was found that tube size and rotation effects were less than 1% in this range.

3. Theory

In order to illustrate the effect we are considering, and before proceeding with the analysis, we present figure 2 which shows the change in the boundary layers at a given streamwise station with zero, positive (suction-side) and negative (pressure-side) rotations. Also shown is the standard log law given by

$$\frac{U}{U_\tau} = \frac{1}{\kappa}\ln\left(\frac{yU_\tau}{\nu}\right) + A; \tag{3.1}$$

here U_τ is the wall-shear velocity given by $U_\tau = (\tau_w/\rho)^{1/2}$ and τ_w is the wall shear stress. The values of the universal constants κ and A are assumed (where necessary)

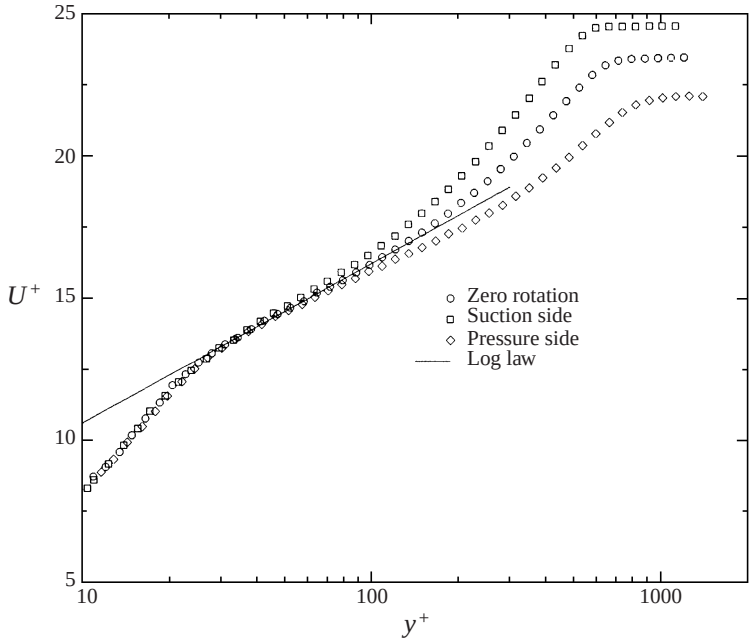

FIGURE 2. Example of effect of rotation on mean velocity profiles.

to be 0.41 and 5.0 respectively. It should be noted that quantities non-dimensionalized using ν and U_τ will be given the superscript + and hence $U^+ = U/U_\tau$ and $y^+ = yU_\tau/\nu$. These profiles are taken from Macfarlane, Joubert & Nickels (1998) for zero-pressure-gradient flow with a free-stream velocity of $10\,\mathrm{m\,s^{-1}}$ at a streamwise position 990 mm from the trip wire and for rotation rates of $-2\pi, 0$ and 2π radians $\mathrm{s^{-1}}$. It may be noted that there is an increase in the profile on the suction side and a decrease on the pressure side relative to the zero-rotation case. The discussion of this behaviour forms the subject of the present work.

Dimensional analysis may be applied to this problem in order to examine the correct relationships among the variables. The derivation of the logarithmic velocity variation in a turbulent boundary layer is considered. In general we have

$$U = f_1(y, U_\tau, \nu, \delta, U_1), \tag{3.2}$$

where U is the velocity at some distance y normal to the wall, U_τ is the wall shear velocity, ν is the kinematic viscosity, δ is the boundary layer thickness and U_1 is the free-stream velocity at the edge of the layer. Where needed, the boundary layer thickness will be taken as the 99.5% thickness, i.e. the distance from the wall, y, at which the velocity first reaches 99.5% of the free-stream velocity, U_1. Let us then suppose that if the Reynolds number is high enough then there will be a region within the layer, away from the wall, where the effect of viscosity on the 'mean relative motions' is insignificant. Let us suppose further that if this region is sufficiently far from the edge of the layer that the 'outer variables', U_1 and δ have an insignificant effect. We are then led to the conclusion that within this region

$$\frac{\partial U}{\partial y} = f_2(y, U_\tau) \tag{3.3}$$

and hence non-dimensionalizing

$$\frac{y}{U_\tau}\frac{\partial U}{\partial y} = \frac{1}{\kappa}, \tag{3.4}$$

where κ is the usual von Kármán constant. Integration of (3.4) then leads to the logarithmic law,

$$\frac{U}{U_\tau} = \frac{1}{\kappa}\log\left(\frac{yU_\tau}{\nu}\right) + A, \tag{3.5}$$

where A and κ are universal constants as noted earlier.

In the case of rotation we can postulate a similar region where the effects of viscosity and the outer variables are negligible but we must include an extra variable Ω, the rotation rate. This then leads to

$$\frac{y}{U_\tau}\frac{\partial U}{\partial y} = f_3\left(\frac{\Omega y}{U_\tau}\right). \tag{3.6}$$

To simplify notation we will define this new parameter as

$$\xi = \frac{\Omega y}{U_\tau}. \tag{3.7}$$

The form of this function is not defined by the above analysis but the analysis of Galperin & Mellor (1991) and of Bradshaw (1969) suggest that it may be Taylor series expanded. To ensure consistency with the non-rotating case, we assign the zeroth-order term the same value, then

$$\frac{y}{U_\tau}\frac{\partial U}{\partial y} = \frac{1}{\kappa} + \beta\xi + \text{h.o.t.}, \tag{3.8}$$

where β is a universal constant. If we drop the higher-order terms (h.o.t.) then integrate we find

$$\frac{U}{U_\tau} = \frac{1}{\kappa}\log\left(\frac{yU_\tau}{\nu}\right) + A + \beta\xi + B(\Omega^+), \tag{3.9}$$

where B is a constant of integration that must depend on Ω^+, which is the appropriate rotation parameter close to the wall based on wall variables defined by

$$\Omega^+ = \frac{\Omega\nu}{U_\tau^2}. \tag{3.10}$$

This is a ratio of the viscous length scale to a rotation length scale, i.e. U_τ/Ω and we shall refer to Ω^+ as the 'viscous rotation parameter'. We would expect the constant β to be universal since we have assumed that no other parameters apply in this region. It should be pointed out that it is not possible to decide *a priori* on the importance of the higher-order terms. The approach adopted here is to examine the empirical results in order to see how well the profiles fit the proposed correction.

If the above analysis holds, and we subtract the mean velocity profiles in the rotating case from the zero-rotation case, we expect to see a universal linear region in all the profiles with a vertical shift which depends on Ω^+. Further, we would expect this region to correspond with the region in which the log law applies, since the reasoning is analogous.

In fact we can make an estimate of the region over which this should apply. Close to the wall dimensional analysis suggests the functional form should be

$$U^+ = f(\xi, \Omega^+), \tag{3.11}$$

and for U^+ to depend on only the first parameter the ratio of the two should be sufficiently large, i.e. greater than some number C, which leads to

$$y^+ > C \tag{3.12}$$

which is the same condition as we expect for the existence of the log law. Examination of boundary layer data suggests that $C \approx 30$ for boundary layers without rotation. In the outer region, if we assume that U_τ is still the relevant velocity scale then an appropriate rotation parameter would be $\Omega_\delta = \Omega\delta/U_\tau$. We would expect that the ratio of ξ to this number should be less than some number D for the arguments to apply, hence

$$\frac{y}{\delta} = \eta < D \tag{3.13}$$

which is the same limit used to define the end of the logarithmic region. The data suggest that $D \approx 0.25$. It should be noted that Coles' law of the wake suggests that the outer limit should also depend on the size of the wake factor Π which is known to be a function of pressure gradient. As Π increases, the effect of the wake penetrates further into the layer. Nevertheless, for flows where the change in the wake parameter is small, the limit is a reasonable first approximation. Examination of the extent of the logarithmic region in the data discussed in this paper suggests that these limits are reasonable.

It is relevant to ask what the behaviour of this extra term is very near the wall, i.e. below our limit of $y^+ = 30$. Consider the Taylor series expansion of the velocity profile near the wall. The first term of this series is

$$U^+ = y^+ \tag{3.14}$$

which follows only from the definition of the wall shear stress. Hence at the wall the effect of rotation does not appear explicitly. It may (and does) affect the value of the wall shear stress but it cannot explicitly affect the first term. In order to conduct a more extensive expansion we consider the boundary layer momentum equations. These have been presented by Johnston, Halleen & Lezius (1972) and for a steady boundary layer may be written as

$$U\frac{\partial U}{\partial x} + V\frac{\partial U}{\partial y} - 2\Omega V = -\frac{1}{\rho}\frac{\partial P^*}{\partial x} + \frac{1}{\rho}\frac{\partial \tau}{\partial y} \tag{3.15}$$

and

$$2\Omega U = -\frac{1}{\rho}\frac{\partial P^*}{\partial y} - \frac{\partial \overline{v'^2}}{\partial y}, \tag{3.16}$$

where the upper-case letters refer to time-averaged quantities and P^* is the reduced pressure defined by $P^* = P - \frac{1}{2}\rho\Omega^2 r^2$, r being the distance from the axis of rotation. Since the centrifugal force is conservative then it is usual to combine it with the static pressure in this way since it has no direct effect on the dynamics of the flow. It is possible to integrate the second equation and substitute it into the first, and with the application of continuity this leads to

$$U\frac{\partial U}{\partial x} + V\frac{\partial U}{\partial y} = -\frac{1}{\rho}\frac{\mathrm{d}P_o^*}{\mathrm{d}x} + \frac{1}{\rho}\frac{\partial \tau}{\partial y}, \tag{3.17}$$

where P_o^* is the reduced static pressure at the wall and we have dropped the small terms which correspond to streamwise derivatives of turbulence intensities. This simple analysis is repeated here since there appears to be an error in Johnston *et al.* (1972).

Their equation (4) is dimensionally incorrect and is also made more complicated by the choice of the pressure at the edge of the layer as the constant of integration. The analysis used here demonstrates the fact that the rotation does not enter explicitly into the equation for the streamwise momentum. The form of (3.17) is also useful when examining the present results (and others) since the pressure gradient is measured via static pressure taps on the wall. The equation is then no different from the standard momentum equation for boundary layers without rotation and hence the series expansion should be the same. The series expansion is reasonably well known and is given by

$$U^+ = y^+ - \tfrac{1}{2}P_o^{*+}y^{+2} + a_3 y^{+4} + \text{h.o.t.} \tag{3.18}$$

where P_o^{*+} is the reduced pressure gradient at the wall non-dimensionalized with wall variables. The first two terms of the series are identical to the zero-rotation case but the constant a_3 depends on terms involving the streamwise derivative of the wall shear stress, the streamwise derivative of the streamwise component of the turbulence intensity and a term proportional to the Reynolds shear stress. The first two terms of the series are identical to the zero-rotation case but the constant in the third term can change since the equations for the evolution of the Reynolds shear stress and the turbulence intensities contain extra terms for production which explicitly involve the rotation. Series expansion of the transport equation for the Reynolds shear stress suggests that, to lowest order, a_3 should include an extra term proportional to the viscous rotation parameter Ω^+ (since the evolution equation contains an extra 'production' term proportional to Ω). Hence we can infer that, if we take the difference of U^+ in the rotating case and in the stationary case in the near-wall region, the first term in the expansion should be at least of order y^{+4} and should be proportional to Ω^+. We also know that this function must asymptote to $\beta\xi + \text{constant}$ for $y^+ > 30$ and so we can construct a plausible form of the inner function as

$$\Delta U^+ = \beta\Omega^+ \frac{y^{+4}}{(y_c^+ + y^+)^3}, \tag{3.19}$$

where y_c^+ represents a 'corner' point where the function changes from fourth order in y^+ to linear. This function asymptotes to y^{+4} as $y^+ \to 0$ and $\beta\xi - 3\beta\Omega^+ y_c^+$ for large y^+. The choice of this corner may be made empirically but it should be such that beyond $y^+ \approx 30$ the function becomes linear. A useful definition of the corner, which is directly related to the sub-layer thickness, is the point at which the production is a maximum. This is found empirically to be around $y^+ = 11$ and hence is the value assumed for the corner. This leads to a constant of $B(\Omega^+) = 33\beta\Omega^+$.

The constant term can also be arrived at by noting that the departure of the profiles from a universal form very close to the wall appears to occur at a fixed value of y^+. Examination of the experimental results suggests that the rotating profiles depart from the stationary profiles close to the point $(U^+, y^+) = (13.7, 35)$. If we denote this point by (U_o, y_o) then

$$U - U_o = \frac{U_\tau}{\kappa}\ln(y) - \frac{U_\tau}{\kappa}\ln(y_o) + \beta\Omega(y - y_o), \tag{3.20}$$

where the constant of integration has been removed by subtracting the two profiles. Non-dimensionalizing and rearranging this becomes

$$U^+ = \frac{1}{\kappa}\ln(y^+) - \frac{1}{\kappa}\ln(y_o^+) + \beta\xi - \beta\Omega^+ y_o^+ + U_o^+. \tag{3.21}$$

Substituting the empirical values for (U_o^+, y_o^+) then leads to

$$U^+ = \frac{1}{\kappa}\ln(y^+) + \beta\xi + 5 - 35\beta\Omega^+, \tag{3.22}$$

which is close to the form found before from a consideration of the near-wall expansion. While this approach is simpler than that given previously it gives no explanation of why the innermost flow is largely unaffected by the rotation. The previous analysis demonstrates the basic form of the correction in terms of its series expansion.

3.1. *Clauser chart*

The excellent fit of this functional form to the data (shown later) suggests that a modified Clauser chart could be constructed as a means of evaluating the skin friction from the mean velocity profiles. This would take the form

$$\frac{U}{U_1} = \frac{1}{S}\left[\frac{1}{\kappa}\ln(R) + \frac{1}{\kappa}\ln(1/S) + A\right] + \beta\frac{\Omega v}{U_1^2}[R - 33S], \tag{3.23}$$

where $R = yU_1/v$, and the procedure would be to plot U/U_1 versus R and adjust $S = U_1/U_\tau$ to find the best fit in the appropriate region. Once S is known the skin friction is known since $S = \sqrt{2/C_f'}$. The classical approach is of course to plot a family of curves for different values of S and then plot the empirical results on this chart, in order to find the line of best fit to the data.

4. Results

The above analysis suggests the existence of a logarithmic region. The results shown here are for boundary layers of low-to-moderate Reynolds numbers. There is some question as to the existence of a log law at these low Reynolds numbers. In response to a request from a reviewer we show here the evidence for the possible existence of a logarithmic region. The most convincing way to demonstrate the existence of such a region is to plot $y^+(\mathrm{d}U^+/\mathrm{d}y^+)$ versus y^+. If a logarithmic region exists, the plot should exhibit a plateau. The problem with this approach is that it requires the differentiation of experimental data which are inherently noisy (despite the best efforts to ensure converged data). In order to overcome this problem the profiles were first smoothed using a three-point running average. The effect of this is similar to a short-wavelength filter and helps to remove random measurement errors. There are around forty points in each profile and hence the smoothing does not alter the shape of the profiles significantly. The results for the zero-rotation profiles of Macfarlane *et al.* (1998) are shown in figure 3. Their parameters are given in Appendix B. There does appear to be a short plateau in the results but the existence of a logarithmic region is arguable. It should be pointed out that it is difficult to achieve high Reynolds number boundary layers subject to system rotation in the laboratory due to limitations on the size of the apparatus. Despite the low-to-moderate Reynolds numbers it will be shown that a linear correction of the form derived appears to be appropriate. It should be noted also that the logarithmic form is not assumed when analysing the profiles.

The following plots are produced by subtracting the profiles subjected to rotation from the zero-rotation profiles at the same streamwise location. A cubic-spline interpolation was used in order to account for the different spacing of the points on the

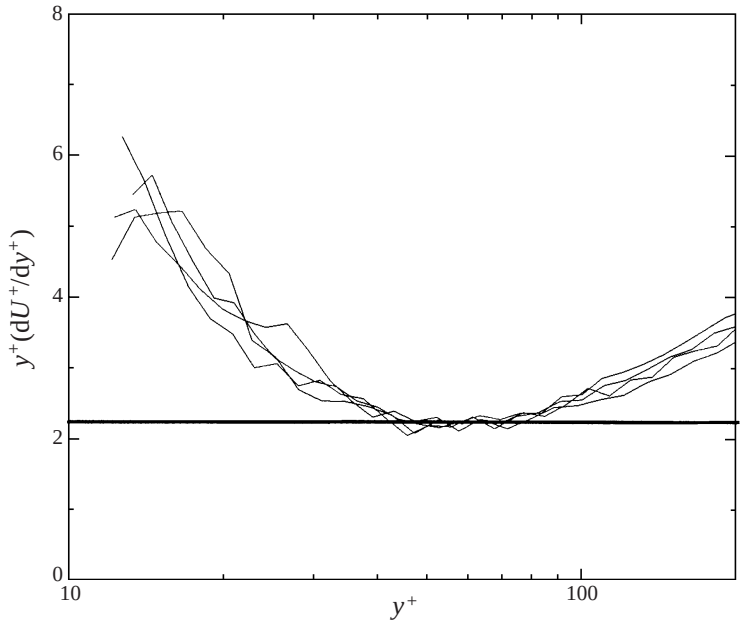

FIGURE 3. Test of existence of logarithmic region for the zero-rotation profiles of Macfarlane *et al.* (1998).

profiles. Previous analyses of data (e.g. Watmuff *et al.* 1985; Bradshaw 1969) have assumed a logarithmic law for the zero-rotation profiles and subtracted this assumed functional form from the rotating profiles. The present approach makes no *a priori* assumption about the existence of a logarithmic region or the values of the constants (κ and A). Also, the present approach should reduce the effect of any consistent errors or offsets in the measurements. We are simply examining the difference between the rotating and non-rotating mean velocity profiles so as to ascertain the effects of rotation. In order to make the process of evaluating the value of the gradient, β, more objective, a least-squares linear fit was made to the data in the region $y^+ > 35$ and $\eta < 0.22$. Since rotation changes the thickness of the boundary layer the minimum value was used as a conservative means of finding the upper limit of the universal region.

Figure 4 shows the results of this procedure applied to the profiles of Macfarlane *et al.* (1998). The magnitude of the gradient is plotted versus Ω_δ and no trend with rotation is apparent. The results support a value of $9.7 \pm 8\%$ with an RMS error of about $\pm 5\%$. The reason for looking at these results in particular is that the data files were directly available, whereas for the results of Watmuff *et al.* (1985) and Ibal (1990) they were measured from printed plots using computer software and so involve some extra error. For comparison a plot of the gradient evaluated by this process for all of the zero-pressure-gradient data available is shown in figure 5. The scatter is much larger but nevertheless supports the conclusion that β shows no significant trend with rotation. The mean of the data in this plot is 10.0 with an RMS error of $\pm 9\%$. It should be noted that these values were obtained objectively without additional subjective input. Visual examination of the fit for the profiles resulting in the outlying points generally shows a poor fit with large scatter. These results were still included in order to be objective. Another crucial point to note is that moderate

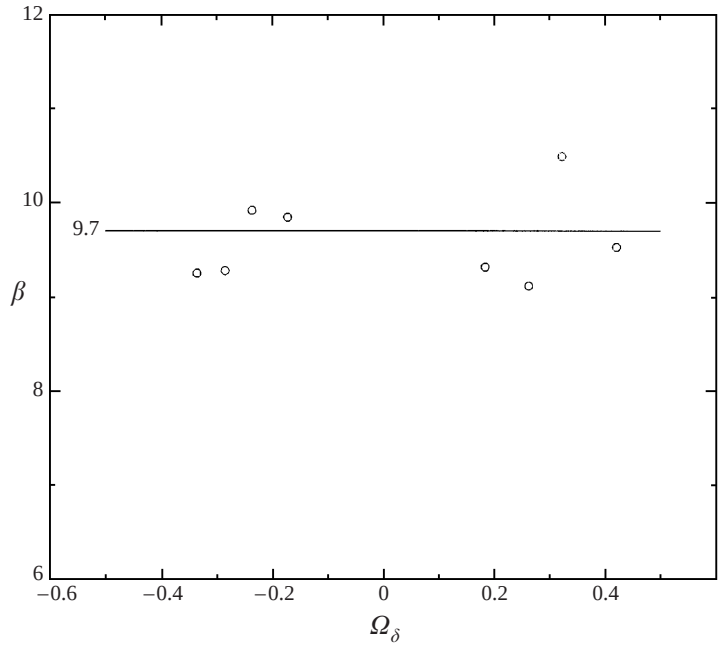

FIGURE 4. Gradient of similarity region ($y^+ > 33$, $\eta < 0.22$) for results of Macfarlane *et al.* (1998).

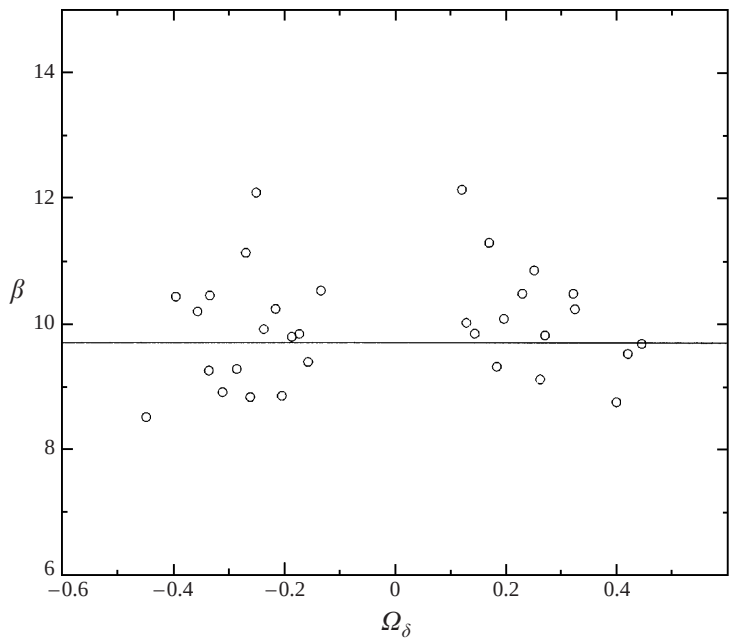

FIGURE 5. Gradient of the linear correction in the region ($y^+ > 33$, $\eta < 0.22$): all zero pressure-gradient studies.

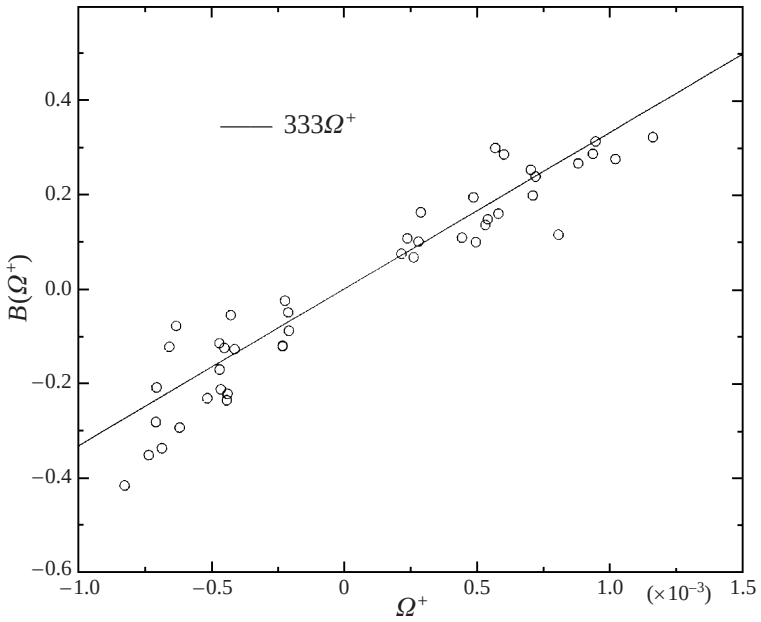

FIGURE 6. Intercept of the linear correction in the region ($y^+ > 33$, $\eta < 0.22$): found assuming a gradient of 9.7: all zero-pressure-gradient studies.

errors in the value of the constant lead to fairly small errors in the velocity profile. The reason is that in this region U^+ varies from approximately 14 to 17. The largest value of ΔU^+ in the region is approximately 2 for this range of rotation and hence the worst error in U^+ is approximately 1%.

In order to examine the behaviour of the constant, $B(\Omega^+)$, in the similarity region, all profiles were fitted with a line $9.7\xi + B$ in this region using least-squares curve-fitting procedure. The result is shown in figure 6. The constant is sensitive to errors and, as a result, there is a large scatter in the data. Nevertheless least-squares curve-fitting of a line to this data gives $B = 333\Omega^+$ as shown on the plot with an RMS error of $\pm 5\%$. This may be compared to the value suggested by the analysis which is $3\beta y_c^+ \Omega^+$ and using the values $\beta = 9.7$ and $y_c^+ = 11$ suggested predicts $B = 320\Omega^+$. It should be emphasized that the values of β and y_c^+ were chosen before these data were plotted and the very close agreement came as a pleasant surprise to the authors.

Having found, in an objective manner, that the conclusions from the analysis are reasonable, the collapse of the data for a series of different experiments is displayed. These profiles were derived as discussed above, i.e. by subtracting the profiles with rotation from the zero-rotation profiles at the same streamwise location. The profiles were first normalized in the standard 'universal' form of U^+ versus y^+ which results in a collapse in the region close to the wall. Shown first are the profiles of Macfarlane *et al.* (1998) since these are the most accurate. The profiles have also been shifted according to the value of the constant, $B(\Omega^+)$, calculated from the theory. This means that the linear region should pass through the origin and the profiles should collapse in the similarity region onto the line $\Delta U^+ = \beta\xi$. Figure 7 shows the profiles from the suction-side boundary layers and it may be noted that the collapse in the inner region is excellent, with the profiles peeling off from the universal law later as the rotation number increases. On this and later plots the number adjacent to each curve is the value of the outer rotation parameter, $\Omega\delta/U_\tau$, which gives the reader a measure of

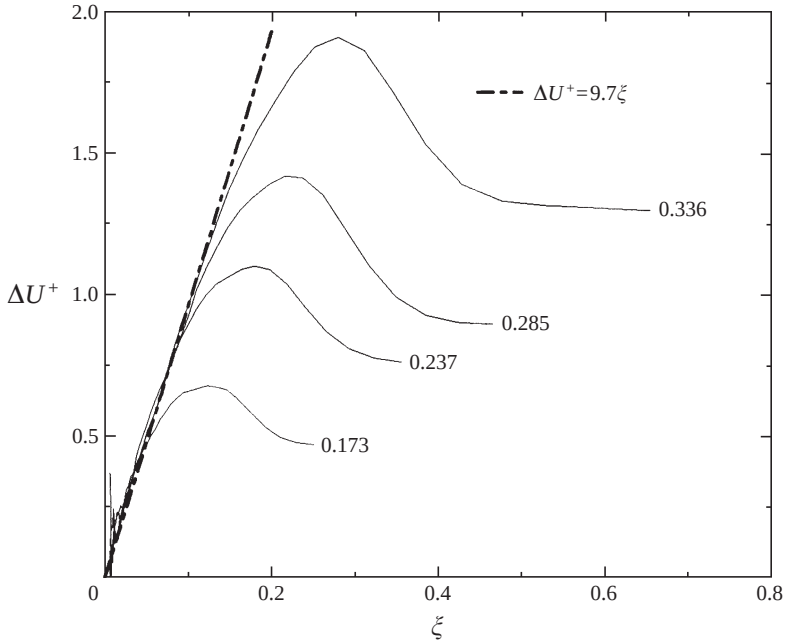

FIGURE 7. All profiles from the suction-side wall for the zero-pressure-gradient measurements of Macfarlane *et al.* (1998).

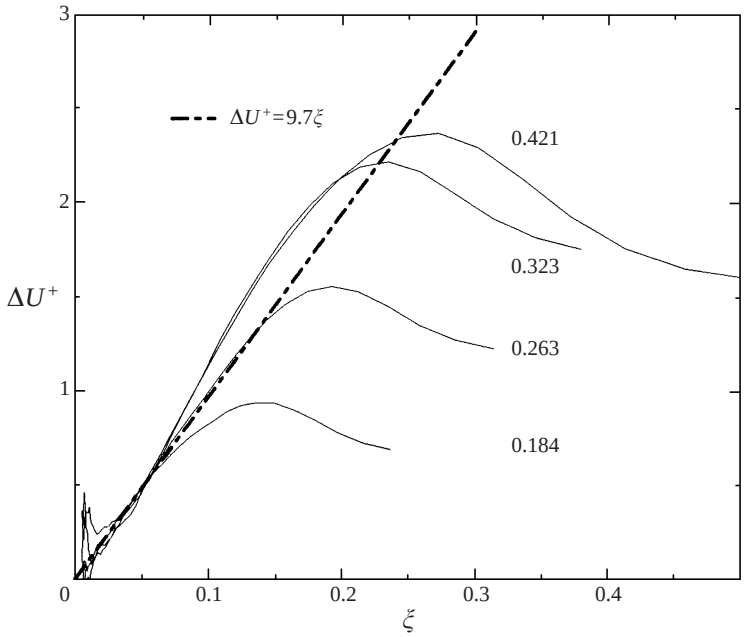

FIGURE 8. All profiles from the pressure-side wall for the zero-pressure-gradient measurements of Macfarlane *et al.* (1998).

the strength of rotation. As a general rule this parameter increases with streamwise distance. The noise in the profiles very near the wall arises from subtracting large numbers that are almost equal.

Figure 8 shows the pressure-side results. Although the difference between the

pressure-side and the zero-rotation profiles is negative they will be shown as positive, i.e. we plot $-\Delta U^+$ for ease of comparison with the suction-side profiles. Again we have a good collapse in the inner region although in this case the profiles appear to peel off to the left of the universal line, i.e. they are above the line, whereas for the pressure side the peel-off is to the right of the line. This is due to the change in δ^+ which occurs as a consequence of rotation. The difference in δ^+ also leads to the characteristic hump in the outer region. The outer flow will be considered later but it is worth noting that dimensional analysis suggests the more appropriate non-dimensional wall distance in this region is y/δ where δ is the boundary layer thickness. This is of course no different to the situation in boundary layers without rotation effects. A point that should be stressed here is that some readers may be tempted to conclude that the pressure-side profiles would be better fitted to a line with a larger value of β since they peel off above the line suggested here. It is important to realize that the linear region should only apply below $\eta \approx 0.25$ and any attempt to fit it beyond this region would lead to misleading results. This may be the reason why some researchers have suggested different empirical constants for stabilized and destabilized flows (i.e. different β). The results presented here suggest that the constant does not depend on the sign of rotation. Over fifty profiles have been plotted in this form and all show a similar collapse onto the universal line. Among them were the profiles of Watmuff *et al.* (1985) for a range of different Reynolds numbers.

It is also interesting that the value of the constant suggested in Bradshaw (1969) for the suction-side profiles (destabilized) is approximately 9, which is close to the value of 9.7 found here.

5. Errors in wall shear stress

In order to establish the validity of the conclusions here a brief discussion of the possible errors in the wall shear stress are discussed.

5.1. *Consistent errors in* U_τ

The calibration of Patel (1965) for the Preston tube was used to calculate the skin friction from the measurements. In the range of the measurements Patel (1964) suggests that the curve-fit to the data given is within $\pm 1.5\%$ of the data. This corresponds to an error in U_τ of $\pm 0.75\%$. This then must be assumed to be the error in U_τ. It will be assumed further that in two given similar flows this error will always be in the same direction as will any small errors in the instrumentation. An error in U_τ of $(1+\epsilon)$ then results in a error in ΔU^+ of $1/(1+\epsilon)$; it will also lead to an error in $\Omega y/U_\tau$ of $1/(1+\epsilon)$ and so in the linear region these errors will tend to cancel and the gradient will be unchanged.

5.2. *Errors of Preston tube measurements due to rotation*

In the majority of the experiments examined here the Preston tube diameter was such that $d^+ = dU_\tau/\nu < 35$ and in this region the effect of rotation was found to be very small, i.e. the mean flow profiles collapsed in this inner region. Thus there should be no direct effect of rotation on the measurement due to a change in the functional form of the mean velocity profile. In fact the functional modification derived here has a negligible effect at these low values of y^+. The other source of potential error arises since the static pressure at the wall was used as a reference for the Preston tube. The potential for error arises since rotation introduces a pressure gradient normal to the

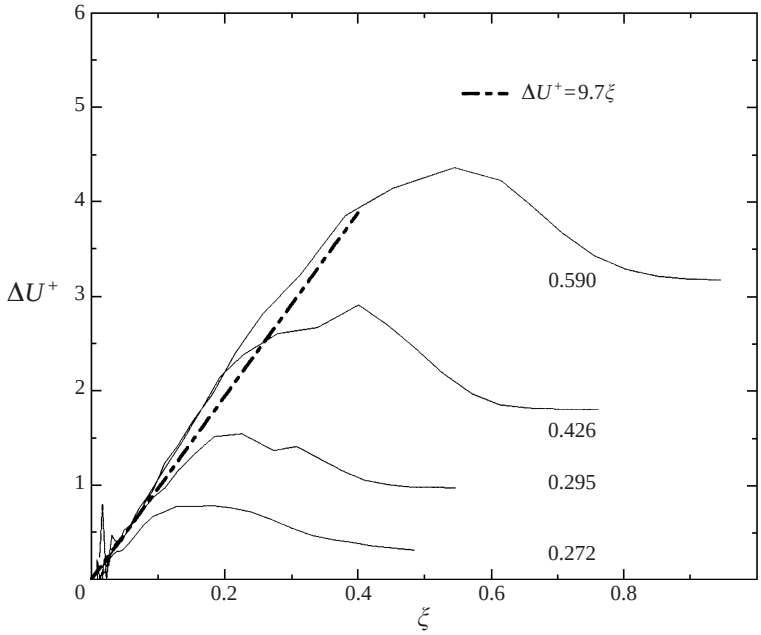

FIGURE 9. All profiles from the suction-side wall for the $10\,\mathrm{m\,s^{-1}}$ adverse-pressure-gradient measurements of Ibal (1990).

wall. As derived earlier this pressure gradient is given to first order by

$$\frac{\partial P}{\partial y} = \rho 2\Omega U(y). \tag{5.1}$$

A conservative (i.e. large) estimate of the error can be made by assuming that the velocity profile is linear throughout this region, i.e.

$$U^+ = y^+, \tag{5.2}$$

which leads to

$$\frac{P - P_o}{P_{dyn}} = 2\Omega^+. \tag{5.3}$$

In the range of values of rotation parameter obtained in these studies the maximum of this error is less than 0.25% and so may be considered negligible. In addition the effect of rotation was examined by measuring the skin friction with different diameter tubes as mentioned previously. The difference was always less than 1%.

6. The effect of added pressure gradient

In order to evaluate the effect of adverse pressure gradient on the 'universal' region the results of Ibal (1990) have been re-analysed. Ibal (1990) studied the effects of rotation on the turbulent boundary layer in a diffusing duct with a 3° included angle. This results in a reasonably strong pressure gradient.

The results are shown in figures 9 and 10. It appears that, even with the addition of a pressure gradient, the universal scaling applies in the inner region. This should not be surprising since the logarithmic law still applies in adverse-pressure-gradient flows and the existence of a universal region here is based on the same assumptions.

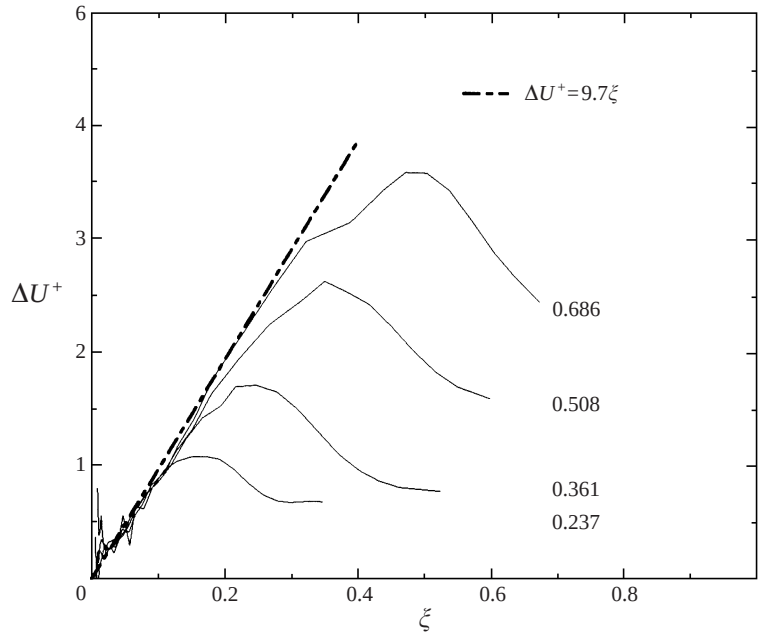

FIGURE 10. All profiles from the pressure-side wall for the $10\,\mathrm{m\,s^{-1}}$ adverse-pressure-gradient measurements of Ibal (1990).

In order to further examine the effect of pressure gradient, mean velocity profiles were measured in an 8° (included angle) rotating diffuser which has an even stronger adverse pressure gradient. The results in figure 11 clearly show a linear region with a constant close to the value of 9.7 suggested.

7. Effect of secondary flow

Rotation of ducts with low aspect ratios leads to the occurrence of secondary flows. This is due to the flow of fluid from the high-pressure side to the low-pressure side along the walls perpendicular to the axis of rotation. These secondary flows can cause significant changes to the mean flow and turbulence quantities. Here we look briefly at some results from a low-aspect-ratio duct to see if the linear correction still applies. The results of Macfarlane *et al.* (1998) for a duct of aspect ratio 1 are shown in figures 12 and 13 for the last streamwise station, where rotation effects are large and secondary flows are also significant. The universal behaviour still applies, although the peel-off is more pronounced on the pressure side. This is not surprising since it has been shown in Macfarlane *et al.* (1998) that the secondary flows introduce streamline convergence on the suction side and divergence on the pressure side. The results of Panchapakesan *et al.* (1997) and Saddoughi & Joubert (1991) on the effect of streamline divergence and convergence on zero-pressure-gradient boundary layers show that divergence increases the skin friction and suppresses the boundary layer growth. The net effect in this case is to increase δ^+ and hence increase the difference in δ^+ between the pressure side and the zero rotation case. On the suction side the net effect is also to increase δ^+ but this brings it closer to the zero-rotation value and hence reduces the difference in the outer flow. This explains the reduced peel-off for the suction-side profiles and the increased peel-off on the pressure side. Figure

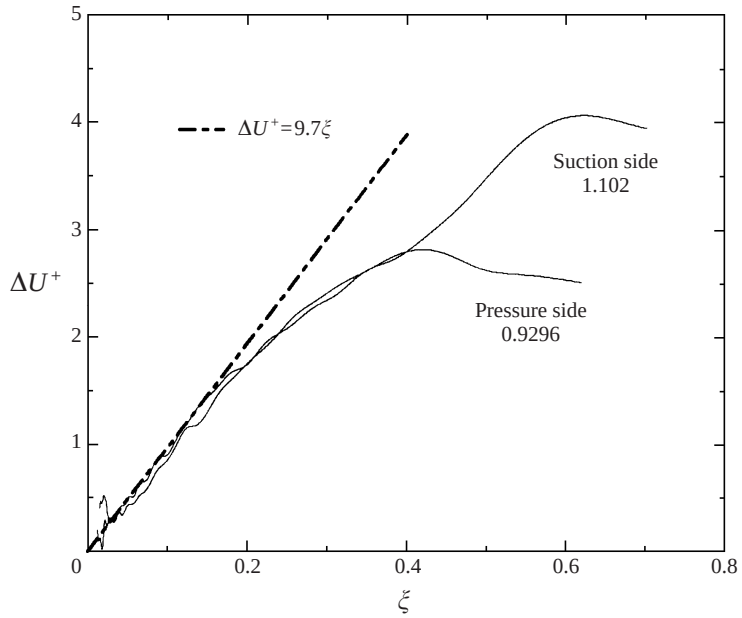

FIGURE 11. Profiles measured in strong (8° included angle diffuser) adverse-pressure-gradient flow for both suction- and pressure-side walls (present results).

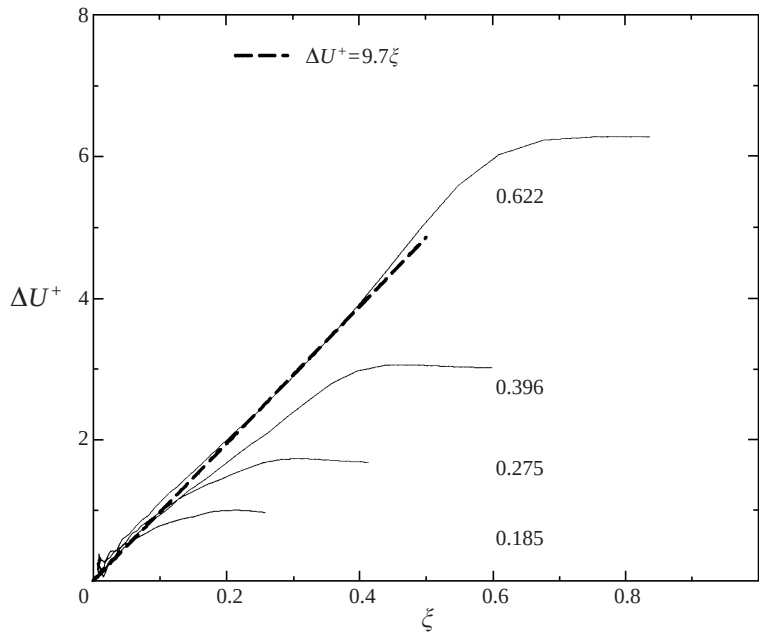

FIGURE 12. Profiles of difference for the suction-side results of Macfarlane *et al.* (1998) for zero pressure-gradient flow in a duct of aspect ratio 1.

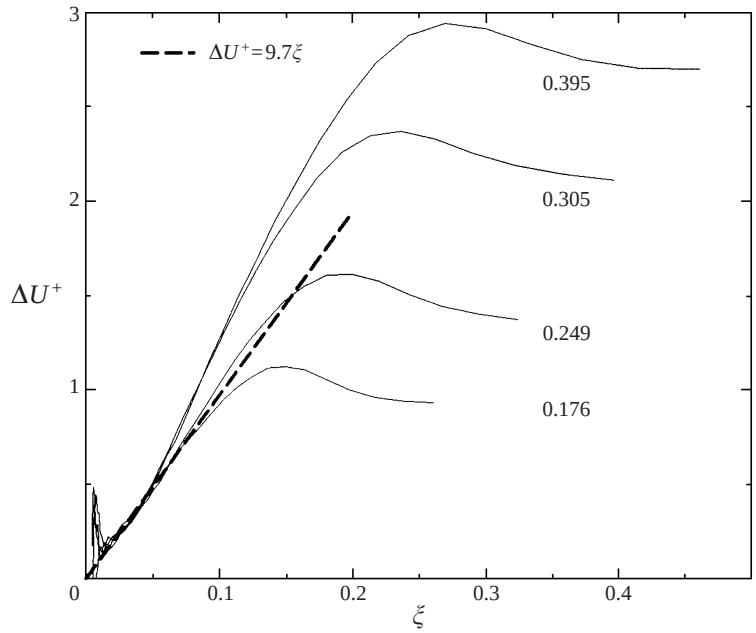

FIGURE 13. Profiles of difference for the pressure-side results of Macfarlane *et al.* (1998) for zero-pressure-gradient flow in a duct of aspect ratio 1.

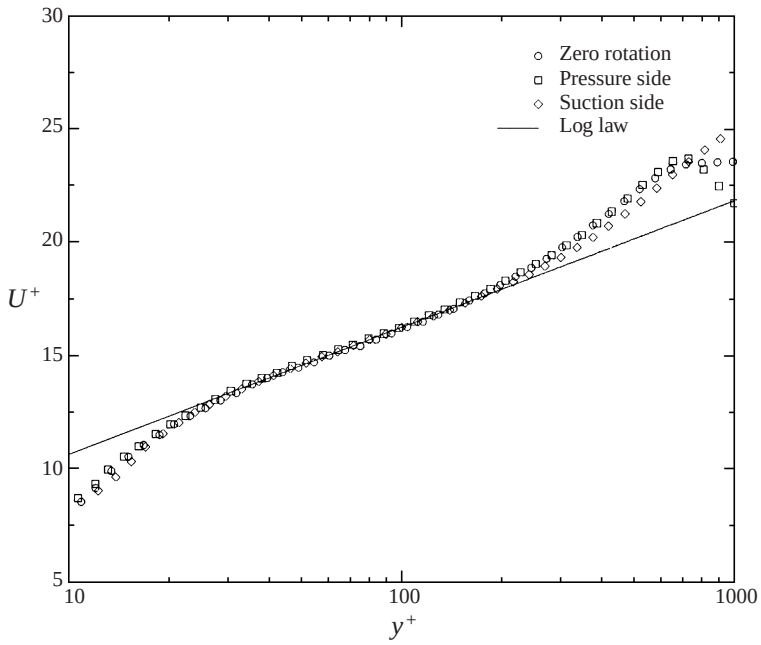

FIGURE 14. Correction applied to profiles with strong secondary flow. Duct of aspect ratio 1, $x = 990$ mm.

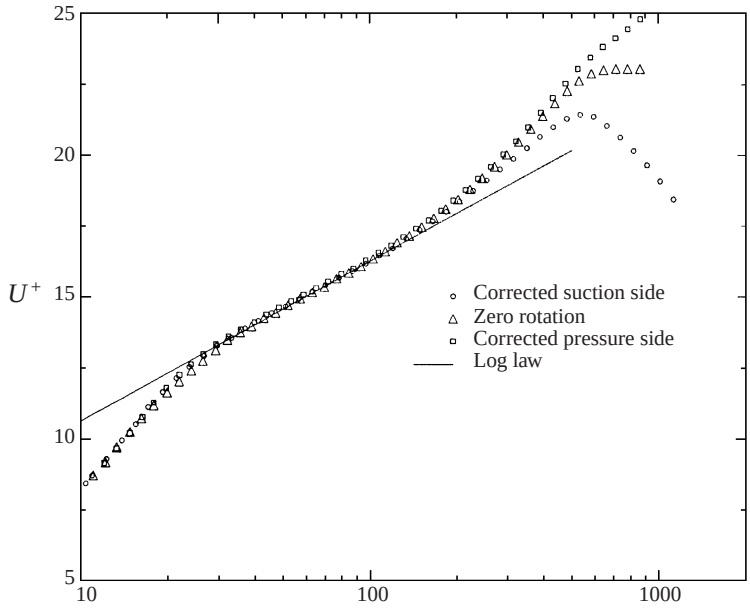

FIGURE 15. Profiles with matched δ^+ with linear correction applied across whole layer.

14 shows the profiles with the correction applied. The collapse is very striking. This flow case is considered a very important test of the universality since the turbulence structure of the flow is modified quite markedly by the secondary flows as will be discussed later.

8. The correction at fixed Reynolds number

It has been noted in the previous sections that the shape of the profiles of ΔU^+ in the outer region is significantly affected by the change in δ^+ that occurs due to rotation. In order to examine the changes in the outer flow in the absence of these effects, profiles have been selected from different streamwise stations so as to match the values of δ^+ for rotating and stationary profiles. In this way it is possible to remove the effect of δ^+ variations and examine the change in the profiles due to rotation alone. Suction, pressure and zero-rotation profiles at the same δ^+ were examined and the proposed correction was removed from the profiles subjected to rotation. In essence then we are removing the effect of rotation and would expect all the profiles to collapse onto the standard log law in the region already defined. The results are shown in figure 15. One interesting feature of this plot is that it appears that the linear correction applies beyond the log region and some way into the outer flow. This extended fit of the linear correction was observed for all profiles examined at fixed δ^+. Naturally it must fail near the outer edge since the velocity attains a constant value. For interest, and in order to allow for this boundary condition, a simple damping was applied to the linear correction of the form

$$\Delta U^+ = (\beta\xi + 33\beta\Omega^+)(1 + (2\eta)^4)/(1 + (2\eta)^5). \tag{8.1}$$

The powers were chosen to provide a rapid approach to a constant value as is obviously necessary from figure 15. Figure 16 shows the result of applying this correction to the same profiles. The results are quite impressive, the only difference

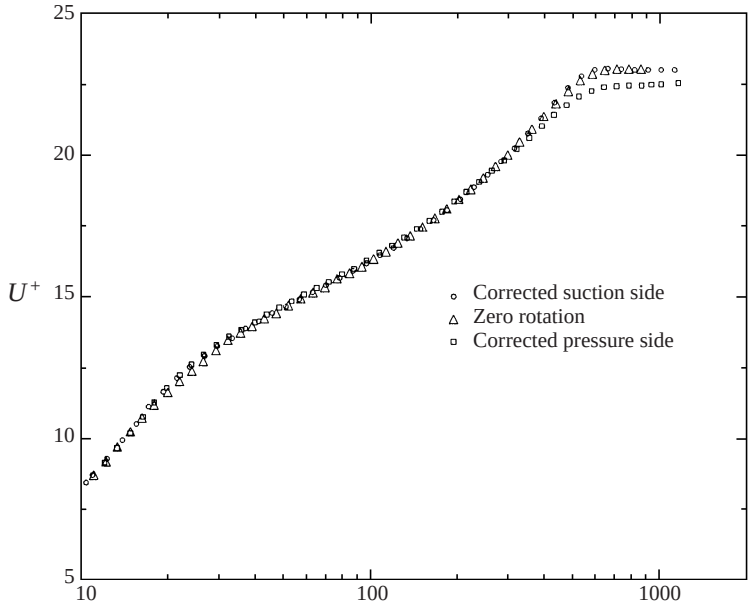

FIGURE 16. Profiles with matched δ^+ with extended correction from (8.1).

between the profiles being a small deficit right at the outer edge. In order to show that the result applies more generally, the same correction has been applied to profiles from an 8° diffuser. The three profiles shown in figure 17 are from the same streamwise station, but due to the nature of the flow the δ^+ values are, nevertheless, approximately matched. The pressure-gradient parameter is also well-matched. The profiles collapse very well over most of the layer.

The observation that the linear correction applies some way into the outer flow for profiles with matched δ^+ is a very interesting result. It suggests that the outer limit for the validity of the correction derived earlier is quite conservative and that the effect of the outer flow scale, δ, on the correction is smaller than was anticipated. The good fit to the profiles with the addition of the empirical damping suggests that the changes in the wake component due to the rotation alone are not large when the Reynolds numbers are matched. It is relevant to note that in low-to-moderate Reynolds number boundary layers it is well known that there is a dependence of Cole's wake factor on Reynolds number. At a fixed streamwise station rotation changes the local Reynolds number and hence may affect the wake component. At fixed Reynolds number this effect has been removed and it appears that changes to the wake component are small.

9. Comment on the value of the constant

The results of this study have given a value for the gradient of the linear correction, β, as $9.7 \pm 8\%$. This corresponds approximately to $8.9 < \beta < 10.5$. Galperin & Mellor (1991) find from their model a value of 7.02. This is approximately 30% lower than the value found here and is well outside the error bounds. Hunt & Joubert (1979) suggested that the value of the constant could be found from a comparison of the ratio of the Reynolds-shear-stress production terms with and without rotation (or in

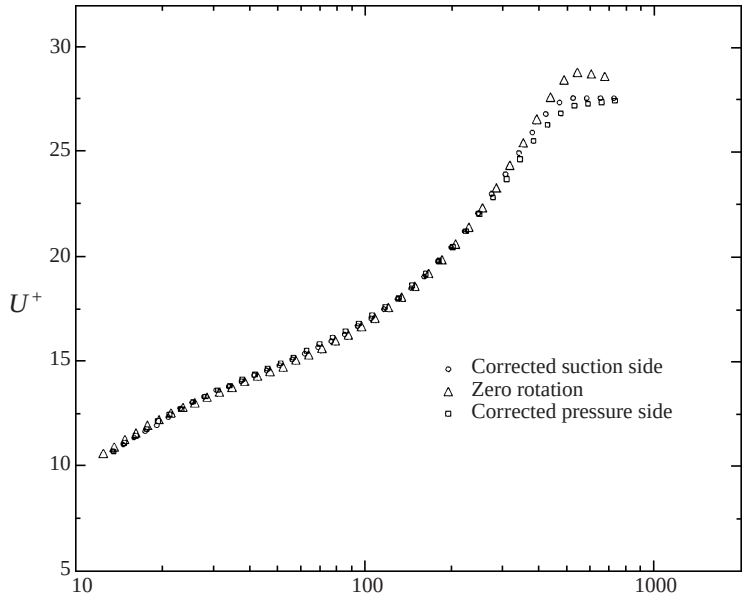

FIGURE 17. Profiles from 8° diffuser with matched δ^+ and extended correction applied from (8.1).

their case curvature effects). This leads to

$$\beta = 2(\overline{u^2}/\overline{v^2} - 1). \tag{9.1}$$

The results of Macfarlane *et al.* give $\overline{u^2}/\overline{v^2} \approx 2.5$ in the outer part of the logarithmic region ($0.15 < \eta < 0.2$) which would give $\beta \approx 3$. If, instead, we take the point of maximum production near the wall then from the simulation of Spalart (1988) $\overline{u^2}/\overline{v^2} \approx 25$ which gives $\beta = 48$. This suggestion then seems flawed in that the value of this 'constant' varies significantly with position through the layer.

The results from the low-aspect-ratio duct emphasize the difficulty of relating the value of β to the turbulence quantities. In particular, the effect of streamline convergence on the suction-side wall leads to large changes in the turbulence quantities near the wall. At the final station for this case the stresses have been reduced by around 30%. Also, the value of $\overline{u^2}/\overline{v^2}$ increases from around 2.5 to 3.5 due to the secondary flows (see Macfarlane *et al.* 1998). Nevertheless the universal linear correction appears to be unaffected. There does not, as yet, seem to be a convincing explanation for either the value of β, or its universality. Like κ it appears to be a universal constant particularly associated with the mean velocity profile.

10. Conclusions

The results and analysis in this paper show that the effect of rotation on the mean velocity profiles of turbulent boundary layers is well-described by a universal linear correction to the logarithmic law. Analysis of a large number of mean velocity profiles under different imposed conditions shows that this linear correction is robust. It does not appear to be affected by Reynolds number (over a limited range), strong adverse pressure gradients or secondary flows. The gradient of the correction term is of the same magnitude for stabilized and destabilized layers. It also appears that

with an appropriate universal damping the linear correction is a reasonably good approximation across the whole layer.

The buffer zone $y^+ < 30$ does not, however, appear to be significantly affected by rotation and the reasons for this have been discussed in terms of the Taylor series expansion of the mean flow. A useful consequence of this is that Preston tubes of diameter $d^+ < 30$ may be used in these flows to measure skin friction.

Appendix A. Comparison to the change in log law constant hypothesis

After analysing their results Watmuff *et al.* (1985) proposed that the effect of rotation was to change the value of the von Kármán constant and hence the gradient of the logarithmic region on semi-log paper. The argument for this hypothesis is based on a spring–mass analogy as suggested by Litvai & Preszler (1969) and further extended by Johnston (1974). The details of the analysis will not be repeated here but the authors of this paper do not find the arguments to be very rigorous or convincing. We will first show that the magnitude of their correction is similar to that proposed here and therefore gives a reasonable fit to the data. We then point out why their suggestion is not consistent with the usual dimensional arguments for the existence of the logarithmic region. Watmuff *et al.* (1985) found, using the analogy and empirical results, an expression for the modified von Kármán constant which was

$$\frac{1}{\kappa_r} = \frac{1}{\kappa}(1 + C\Omega^+), \tag{A 1}$$

where κ_r is the new or modified constant and C is another supposedly 'universal' constant to be determined empirically. Now, if it is assumed that, instead, the form suggested in the present work is correct, it is possible to examine what the apparent form of the modified constant would be if this alternative approach were used. In the logarithmic region this leads to

$$\frac{1}{\kappa_r}\ln(y^+) + A_r = \frac{1}{\kappa}\ln(y^+) + A + \beta\xi - 3\beta y_c^+\Omega^+, \tag{A 2}$$

where A is the usual additive constant in the log law ($A = 5$ for the data considered here) and A_r is the constant for the rotating case. Watmuff *et al.* (1985) find the value of A_r by assuming that all profiles coincide at the point $U^+ = 15$, $y^+ = 40$ which leads to

$$A_r = 15 - \ln(40)/\kappa_r. \tag{A 3}$$

Substituting this into (A 2) and using the fact that $\xi = \Omega^+ y^+$ and the value found earlier for y_c^+, leads directly to

$$\frac{1}{\kappa_r} = \frac{1}{\kappa}\left(1 + \kappa\beta\Omega^+\frac{(y^+ - 33)}{\ln(y^+) - \ln(40)}\right). \tag{A 4}$$

This is of the same form as that of Watmuff *et al.* (1985) if the function

$$\frac{(y^+ - 33)}{\ln(y^+) - \ln(40)} \tag{A 5}$$

is approximately constant over the region where the log law applies. The region over which the log law applies in most of their data is approximately from $45 < y^+ < 200$ and the maximum and minimum values of this non linear function over this range

x (mm)	Ω (rad s^{-1})	U_1 (m s^{-1})	δ (mm)	Ω^+ ($\times 10^3$)	Ω_δ	S
300	2π	10	12.7	0.443	0.173	21.7
300	0	10	13.4	0	0	21.4
300	-2π	10	13.9	−0.411	−0.184	20.8
530	2π	10	16.3	0.496	0.237	22.8
530	0	10	17.3	0	0	22.3
530	-2π	10	19.1	−0.438	−0.263	21.2
760	2π	10	18.9	0.540	0.285	23.8
760	0	10	19.7	0	0	23.0
760	-2π	10	23.3	−0.440	−0.323	21.6
990	2π	10	21.4	0.579	0.336	24.6
990	0	10	24.2	0	0	23.4
990	-2π	10	29.7	−0.469	−0.421	22.0

TABLE 1. Parameters for profiles of Macfarlane *et al.* (1998).

are 103 and 68 respectively. If we take the average of this non linear function over the range we find a value of 82, which leads to

$$\frac{1}{\kappa_r} = 2.44 - 795\Omega^+ \tag{A 6}$$

as compared with

$$\frac{1}{\kappa_r} = 2.44 - 750\Omega^+ \tag{A 7}$$

found empirically by Watmuff *et al.* (1985). Hence we have found that the magnitude of the correction they suggested coincides approximately with that of the linear correction derived in this paper.When examined on the usual (U^+, y^+) plot it is difficult to choose between them. Dimensional analysis does, however, suggest a valid criticism of the above form. If we use the form given above it is not difficult to derive an expression for $\partial U/\partial y$ which is

$$\frac{\partial U}{\partial y} = \frac{U_\tau}{\kappa y} + \frac{C\Omega v}{yU_\tau} \tag{A 8}$$

and hence according to this model the 'mean relative motions' are no longer independent of viscosity. It is difficult to understand how the effect of rotation could lead to a dependence of this region on viscosity since it is the independence from viscous effects that leads to the 'log law'. The problem cannot be remedied by choosing Ω_δ as the relevant parameter as this would lead to functional dependence on the outer flow variables. The analysis and empirical results in this paper suggest that the modification of κ by rotation is not justified and a linear correction is better supported by both analysis and experiment.

Appendix B. Table of mean flow parameters for the data

The mean parameters for the data of Macfarlane *et al.* (1998) are presented in table 1.

REFERENCES

Bradshaw, P. 1969 The analogy between streamline curvature and buoyancy in turbulent shear flow. *J. Fluid Mech.* **36**, 177–191.

Erm, L. P. 1988 Low Reynolds number turbulent boundary layers. PhD thesis, University of Melbourne, Australia.

Galperin, B. & Mellor, G. L. 1991 The effects of streamline curvature and spanwise rotation on near-surface, turbulent boundary layers. *Z. Angew. Math. Phys.* **42**, 565–583.

Halleen, R. M. & Johnston, J. P. 1967 The influence of rotation on flow in a long rectangular channel – an experimental study. *Stanford University*, *Dept. Mech. Engng*, *Thermosci. Div. Rep.* MD-18.

Hunt, I. A. & Joubert, P. N. 1979 Effects of streamline curvature on turbulent duct flow. *J. Fluid Mech.* **91**, 633-659.

Ibal, G. 1990 Adverse pressure gradient and separating turbulent boundary layer flows with system rotation. PhD thesis, University of Melbourne, Australia.

Johnston, J. P. 1974 The effects of rotation on boundary layers in turbomachine rotors. In *Fluid Mechanics*, *Acoustics and Design of Turbomachinery*, *NASA SP*-304, pp. 207–249.

Johnston, J. P., Halleen, R. M. & Lezius, D. K. 1972 Effects of spanwise rotation on the structure of two-dimensional, fully developed turbulent channel flow. *J. Fluid Mech.* **56**, 533–557.

Litvai, E. & Preszler, L. 1969 On the velocity profile of the turbulent boundary layer on rotating impeller blading. *Periodica Polytechnica*, *Mech. Engng* **13**, 215–228.

Macfarlane, I., Joubert, P. N. & Nickels, T. B. 1998 Secondary flows and developing, turbulent boundary layers in a rotating duct. *J. Fluid Mech.* **373**, 1–32.

Panchapakesan, N. R., Nickels, T. B., Joubert, P. N. & Smits, A. J. 1997 Lateral straining of turbulent boundary layers. Part 2. Streamline convergence. *J. Fluid Mech.* **349**, 1–30.

Patel, V. C. 1965 Calibration of the Preston tube and limitations on its use in pressure gradients. *J. Fluid Mech.* **23**, 185–208.

Saddoughi, S. G. & Joubert, P. N. 1991 Lateral straining of turbulent boundary layers. Part 1. Streamline divergence. *J. Fluid Mech.* **229**, 173–204.

Spalart, P. R. 1988 Direct simulation of a turbulent boundary layer up to $R_\theta = 1410$. *J. Fluid Mech.* **187**, 61–98.

Watmuff, J. H., Witt, H. T. & Joubert, P. N. 1985 Developing turbulent boundary layers with system rotation. *J. Fluid Mech.* **157**, 405–448.